*Quantum Electronics* **49** (6) 529–534 (2019) ©2019 Kvantovaya Elektronika and Turpion Ltd

https://doi.org/10.1070/QEL17043

# Effect of (Al)GaAs/AlGaAs quantum confinement region parameters on the threshold current density of laser diodes

M.A. Ladugin, A.A. Marmalyuk

*Abstract.* **An approach has been proposed for choosing parameters (width and depth) of an (Al)GaAs/AlGaAs quantum confinement region via calculation of the threshold current density of a semiconductor laser. A detailed assessment of its components has made it possible to find criteria for optimising the range of quantum well widths so as to minimise the threshold current for lasers with different heterostructure geometries. The data presented in this paper demonstrate the feasibility of further improving output characteristics of semiconductor lasers by optimising the design and technology of quantum well heterostructures. Owing to this, we have simultaneously reduced the threshold current, carrier escape and internal optical loss, which has allowed us to obtain high (60 % to 70 %) efficiencies of a semiconductor laser operating in the spectral range 800–850 nm.**

***Keywords:*** *semiconductor laser, threshold current density, GaAs/AlGaAs heterostructure, quantum well.*

## 1. Introduction

Semiconductor laser diodes (LDs) are currently among the most attractive coherent light sources for a variety of applications, because they need low pump currents, offer high external differential efficiency and have a small size. For example, lasers having low operating currents play a key role in those communications applications where signal modulation and high data rate are of critical importance [1]. An improved electrical-to-optical power conversion efficiency is a critical parameter of lasers in technological applications related to materials processing [2]. Long-term and stable operation of a light source often depends on the applied electric current, so high-efficiency, low-pump-current LDs are necessary for resolving most practical issues.

Even though a typical efficiency ($\eta$) of laser diodes and bars has reached about 55 %–60 %, further improvements are needed for a number of applications. Raising efficiency to above 70 % requires an even more effective optimisation of the parameters that appear in the well-known relation

$$\eta = \eta_{\rm d}\frac{h\nu}{q}\frac{I - I_{\rm th}}{I(V_0 + IR_{\rm s})}, \quad (1)$$

**M.A. Ladugin, A.A. Marmalyuk** OJSC M.F. Stel'makh Polyus Research Institute, ul. Vvedenskogo 3, 117342 Moscow, Russia; e-mail: maximladugin@mail.ru

Received 18 April 2019
*Kvantovaya Elektronika* **49** (6) 529–534 (2019)
Translated by O.M. Tsarev

where $\eta_{\rm d}$ is external differential efficiency; $h\nu$ is the emitted photon energy; $q$ is the electron charge; $I$ and $I_{\rm th}$ are the operating and threshold currents, respectively; $V_0$ is the threshold voltage; and $R_{\rm s}$ is the series resistance.

The output characteristics of LDs can be improved by raising their external differential efficiency or reducing their threshold current, internal optical loss, threshold voltage and series resistance [3, 4]. Even a slight improvement in these parameters allows one to finally markedly improve the emission characteristics and efficiency of the devices in question. In particular, an additional reduction in threshold current, operating voltage and internal optical loss in novel (Al)GaAs/AlGaAs laser heterostructure designs by just 5 %–10 % will allow maximum efficiency to be improved by 2 %–5 %, leading to a noticeable reduction in the thermal load on laser bars and arrays [5].

Since most parameters of LDs are set in the epitaxial heterostructure design and growth stages, this paper considers an approach that allows one to optimise the configuration of a quantum confinement active region, which determines the threshold current density and the dependence of optical gain on injection current, for ensuring high output power and efficiency.

## 2. Results and discussion

In analysing threshold current density, we examined a heterostructure with $Al_xGa_{1-x}As$ ($x$ = 0.1–0.5) barrier layers and one (Al)GaAs quantum well (QW), such as are often used in making laser emitters in the popular spectral region 790–860 nm [5, 6]. In the most general case, threshold current density $J_{\rm th}$ is the sum of its components, which can be written as follows [3, 7]:

$$J_{\rm th} = J_{\rm transp} + J_{\rm int} + J_{\rm ext} + J_{\rm spread} + J_{\rm vertleak}$$

$$+ J_{\rm SRH} + J_{\rm surf} + J_{\rm interface} + J_{\rm Auger}, \quad (2)$$

where $J_{\rm transp}$ is the transparency current density; $J_{\rm int}$ and $J_{\rm ext}$ are the current densities needed to compensate for internal and external optical losses, respectively; $J_{\rm spread}$ is the density of the current lost because of the lateral carrier spreading; $J_{\rm vertleak}$ is the density of the current lost because of the carrier escape from the active region; $J_{\rm SRH}$ is the Shockley–Read–Hall recombination current density; $J_{\rm surf}$ is the surface recombination current density; $J_{\rm interface}$ is the current density due to recombination on the heterojunctions; and $J_{\rm Auger}$ is the Auger recombination current density.

Typical threshold current densities ($J_{\rm th}$ ) in conventional high-power LDs based on (Al)GaAs/AlGaAs heterostruc-

tures lie in the range from about 200 to 400 A cm$^{-2}$. Note that, as a rule, the transparency current density ($J_{transp}$) is 130 ± 50 A cm$^{-2}$ and the $J_{int}$ and $J_{ext}$ current densities are 10 ± 5 and 100 ± 50 A cm$^{-2}$, respectively. The other terms in (2), which are sometimes left out of consideration in analysing threshold current density for a number of reasons [8], account for up to 100 A cm$^{-2}$.

In an ideal case, carrier transport can be schematised as shown in Fig. 1a, where vertical and lateral leakages are zero, all possible nonradiative recombination channels are completely eliminated, and there are no internal or external losses (for example, in the case of an infinite cavity and minimum losses due to scattering and absorption by free charge carriers). At the same time, in a real device (Fig. 1b) current losses can be significant, and the minimum theoretical threshold current density will then be exceeded by several times.

The smallest contribution to the threshold current density is made by the transparency current density, $J_{transp}$, at which a necessary transparency of the gain medium of the laser is ensured (the gain is equal to the loss). This condition is known to be fulfilled [9] when the separation between the quasi Fermi levels $E_{Fc}$ and $E_{Fv}$ in the conduction band (CB) and valence band (VB) is equal to the energy difference between accessible size quantisation levels for electrons and holes ($E_e$ and $E_h$) in these bands (transparency condition):

$$E_{Fc} - E_{Fv} \geqslant E_e - E_h. \quad (3)$$

In LDs, this separation between the quasi Fermi levels requires carrier injection via electric current, and a transition from absorption to amplification occurs at a certain carrier concentration, $N_{transp}$, which ensures transparency of the medium. Absorption or amplification prevails, depending on the injected carrier concentration or the probability that VB and CB states are occupied. $N_{transp}$ values typical of (Al)GaAs and InGa(As,P) materials lie in the range $(1-3) \times 10^{18}$ cm$^{-3}$. Indeed, in the case under consideration here, for a GaAs-based QW with a standard width $L_z$ = 10 nm the 3D carrier concentration required for the medium to be transparent is $(1-1.5) \times 10^{18}$ cm$^{-3}$, as estimated using a rough technique described below (Fig. 2). The current density, related to carrier concentration by

$$J_{transp} = qN_{transp}L_z/t_{rec}, \quad (4)$$

is 80–120 A cm$^{-2}$ for the configuration in question at typical radiative lifetimes $t_{rec}$ = 1–3 ns [10, 11]. In most experimental studies [2, 7, 8, 12–19], this current density term, present in (2), is usually not analysed in detail, but is merely determined in a linear or exponential model for the threshold current by

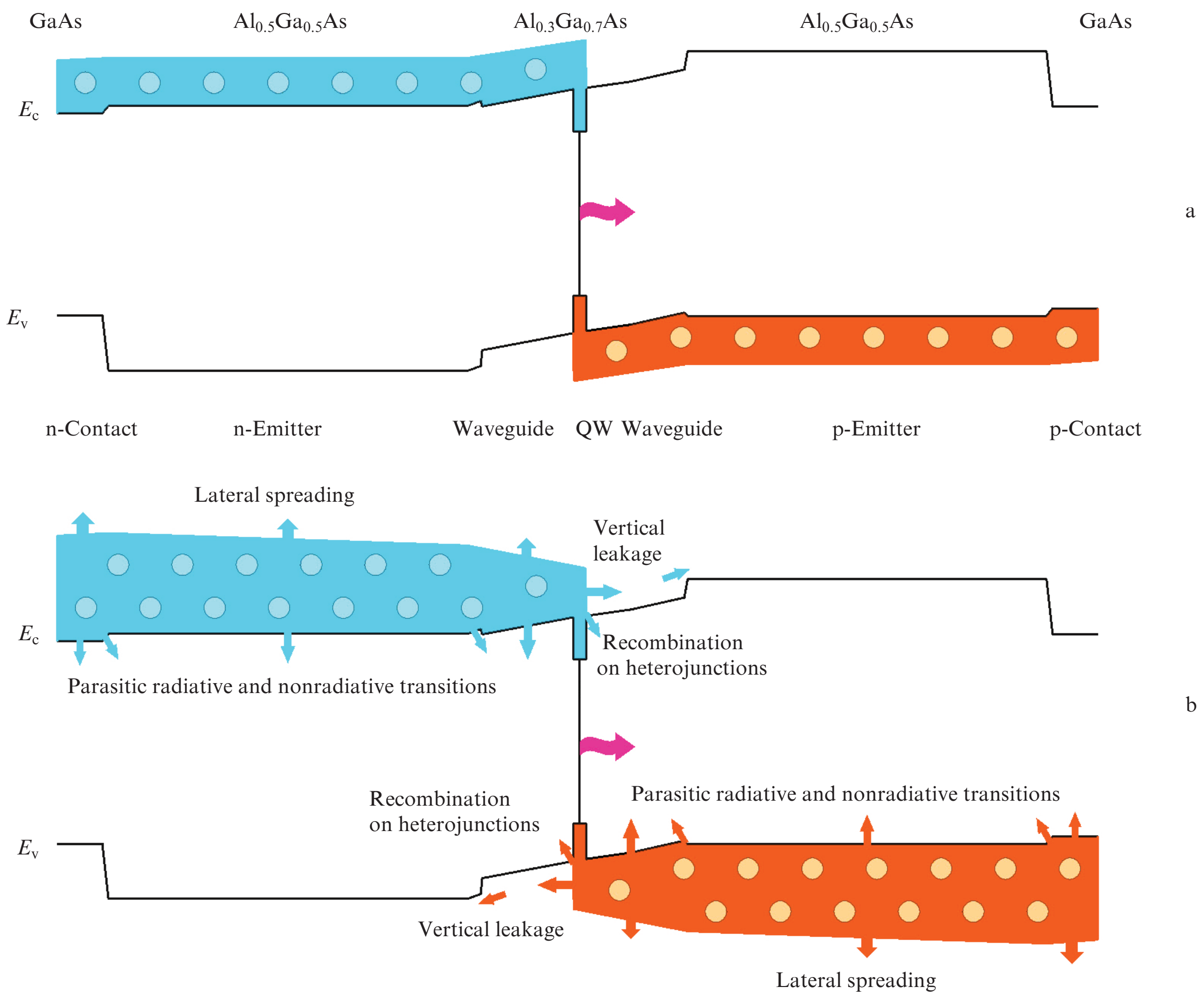


**Figure 1.** Schematic of carrier injection in a quantum-confined laser heterostructure in (a) an ideal and (b) a real case.

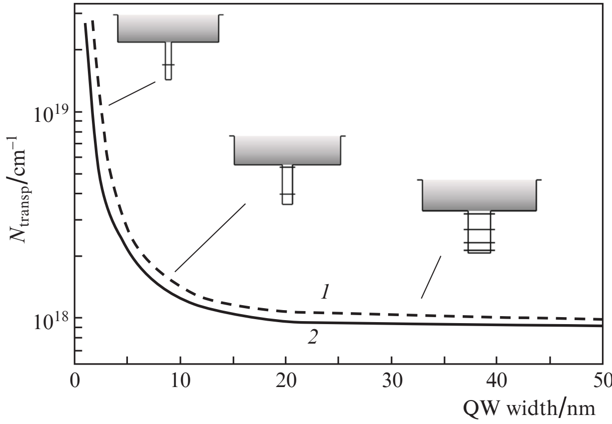


**Figure 2.** 3D transparency concentration as a function of the width of a GaAs QW sandwiched between $Al_xGa_{1-x}As$ barrier layers with $x$ = (1) 0.2 and (2) 0.4. Insets: schematic of the conduction band of the quantum-confined heterostructure used in the calculations.

measuring it for laser diodes differing in cavity length or mirror reflectivity.

The minimum threshold current was calculated in a number of studies [7, 9, 19–22], but they rarely analysed the dependence of the transparency current density on the active region configuration, which is determined by not only the width of QWs and the composition of their material but also the width and composition of the neighbouring barrier layers. For example, only one active region configuration, with fixed QW and barrier compositions, was calculated in each of Refs [9, 19]. In Refs [20] and [21, 22], the minimum threshold current density for similar active region configurations corresponded to QW widths of 6 and 15 nm, respectively, even though there were experimental data. One possible reason for the scatter in results for a given material system is that the measured threshold currents in the above-mentioned studies included all leakage currents, nonradiative recombination currents and currents due to surface recombination on various heterojunctions. A consistent theoretical model for threshold current calculation was proposed by Sugimura [19]. Unfortunately, it is unsuitable for fitting experimental data for laser structures with a QW width under 4–5 nm (e.g. to results reported by Hersee et al. [16] and Lo et al. [17]) because the threshold current calculated for such QW configurations tends to infinity.

To assess the effect of active region parameters on the transparency current density, we considered a standard laser heterostructure configuration [23] consisting of five layers, whose band diagram is shown in the Fig. 2 insets. As cladding layers, we chose an $Al_{0.6}Ga_{0.4}As$ wide-band-gap layer. A QW based on an $Al_xGa_{1-x}As$ ($x$ = 0–0.06) ternary compound was sandwiched between $Al_xGa_{1-x}As$ ($x$ = 0.05–0.5) barrier layers.

To find the current density at which condition (3) is met as a function of quantum confinement active region configuration, it is necessary to determine the position of the quasi Fermi levels in the corresponding subbands using the relations [24]

$$N_{\rm e} = kT\sum_i\left(\frac{m_{\rm c\it i}}{\pi\hbar^2 L_z}\right)\ln\left[1+\exp\left(\frac{E_{\rm Fc}-E_{i\rm c}}{kT}\right)\right],$$

$$N_{\rm h} = kT\sum_i\left(\frac{m_{\rm v\it i}}{\pi\hbar^2 L_z}\right)\ln\left[1+\exp\left(\frac{E_{\rm Fv}-E_{i\rm v}}{kT}\right)\right], \tag{5}$$

where $N_{\rm e,h}$ is the 3D electron and hole concentration; $m_{{\rm c}i,{\rm v}i}$ is the carrier effective mass in the CB and VB; and $E_{i\rm c}$ and $E_{i\rm v}$ are the size quantisation levels in the CB and VB.

The summation should be carried out over all quantised subbands within each band: in the CB, for electrons in the Γ, L, and X minima, and in the valence band, for light and heavy holes. Taking into account the L minima (for $Al_xGa_{1-x}As$ with $x > 0.3$) and X minima (for $Al_xGa_{1-x}As$ with $x > 0.4$) in the CB is particularly important at elevated temperatures or QW widths under 7 nm, i.e. in the cases where filling of high-energy quantum states is the most likely.

The position of the size quantisation energy levels for electrons and holes in the configuration under discussion was determined by solving the steady-state Schrödinger equation for a QW of finite depth, as was demonstrated by Dragunov et al. [25].

The transparency current density was determined for active region configurations with GaAs-based QWs and different $Al_xGa_{1-x}As$ ($x$ = 0.1–0.5) barrier layers. The cladding $Al_xGa_{1-x}As$ layers had $x$ = 0.60. Figure 3 shows the transparency current density as a function of QW width. It is seen from the data obtained that, as the QW width decreases from several tens of nanometres to about 6–7 nm, the transparency current density decreases linearly to ~100 A cm$^{-2}$, before sharply rising at QW widths under 4 nm.

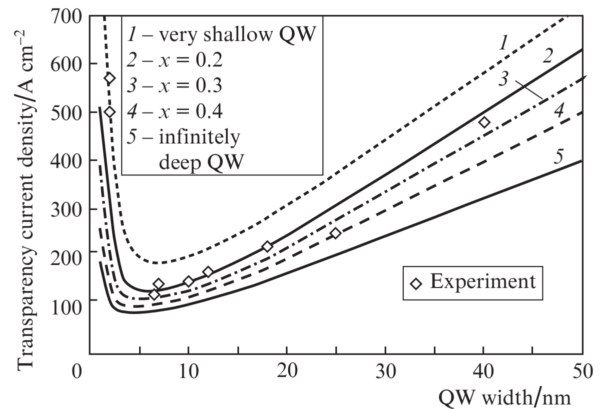


**Figure 3.** Transparency current density as a function of the width of a GaAs QW sandwiched between $Al_xGa_{1-x}As$ barrier layers with different compositions. The open diamonds represent experimental data from Refs [2, 12–14, 16–19, 26].

The initial decrease in current density is due to the presence of a large number of size quantisation levels in QWs 20 to 40 nm in width. At room temperature, higher excited state levels are located below or within $kT$ from the quasi Fermi level in the CB and have considerable population. Therefore, because of the temperature distribution of charge carriers, the excited state levels take off some of the carriers and are parasitic from the viewpoint of efficient lasing.

Zero gain, i.e. the fulfilment of the transparency condition, depends only on the density of the lower quantum state in the corresponding band, a parameter that increases with decreasing QW width. The minimum transparency current density corresponds to a situation where the lower

ground level in the QW is the only level in the potential well and has the maximum separation from the levels in the barrier material. Further decrease in the width of the potential well has a negative effect on carrier confinement in it, so additional injection is needed to ensure zero gain, leading to an increase in transparency current density at QW widths under 4 nm.

In the case of a deeper QW formed by barrier layers with higher $x$ values, injected carriers are better confined in it. It is worth noting that the current density in $Al_xGa_{1-x}As$ barriers with $x > 0.4$ decreases more gradually because of the likely filling of the L and X minima in the indirect band gap material with electrons. In addition, with decreasing QW depth the quasi Fermi level approaches the barrier level or, sometimes, lies above it. This is accompanied by a considerable filling of states in the barrier material, leading to an appreciable carrier loss. The calculated results agree well with experimental data (Fig. 3).

Figure 4 shows the transparency current density calculated for $Al_xGa_{1-x}As$ QWs with different compositions ($x = 0-0.06$) at fixed $Al_xGa_{1-x}As$ barriers with $x = 0.30$. The variation of current density with QW width is similar to that in Fig. 3: reducing the depth of the potential well (by varying the composition of the $Al_xGa_{1-x}As$ in the QW) increases the transparency current density. Note that, with increasing $x$, the minimum in it shifts to larger QW widths.

electron concentration required for achieving transparency of the gain medium can be located beyond the quantum confinement region.

The inefficient carrier capture in wells less than 5 nm in width [27, 28] during laser operation leads to an appreciable current leakage ($J_{vertleak}$) to the barrier layers and an increase in internal optical loss.

To assess carrier capture efficiency in AlGaAs QWs emitting at a wavelength near 800 nm, we carried out a number of experiments. As barrier layers, we chose $Al_xGa_{1-x}As$ with $x = 0.3$, and the QW width was varied from 4 to 12 nm. Measuring the intensity of photoluminescence spectra of our samples, we obtained one minimum, near 9 nm, and two maxima, near 5.5 and 11 nm (Fig. 5). From the quantum-mechanical point of view [29], the reason for this behaviour is that the electron capture probability increases when a new size quantisation level emerges in the well. In the example considered above, this state just corresponds to QW widths of 5.5 and 11 nm. At the same time, as pointed out by Haverkort et al. [30] the concentration of injected carriers during laser operation considerably exceeds the carrier concentration due to optical excitation, so such oscillations in measurements of output characteristics of laser diodes can be less pronounced. Nevertheless, in designing an efficient quantum confinement region, it is necessary to take into account the effect of QW parameters on the capture rate [28–31].

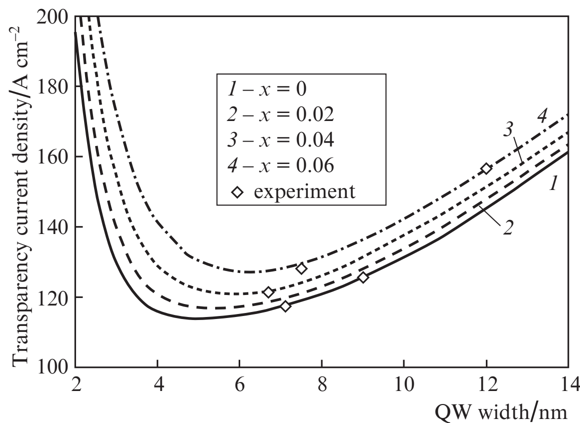


**Figure 4.** Transparency current density as a function of the width of $Al_xGa_{1-x}As$ QWs with different compositions ($x = 0-0.06$) sandwiched between $Al_{0.3}Ga_{0.7}As$ barrier layers.

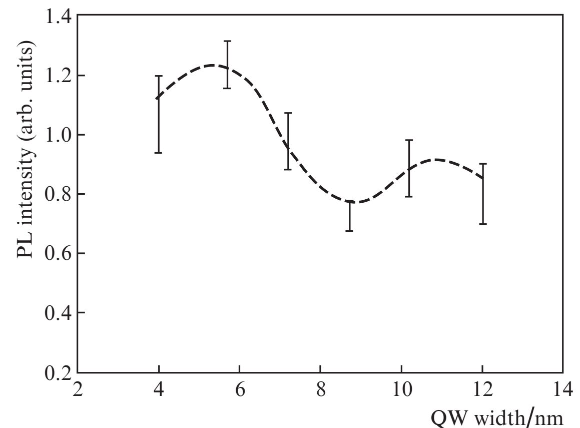


**Figure 5.** Photoluminescence intensity as a function of the width of AlGaAs QWs emitting at a wavelength of 800 nm.

In analysing the carrier distribution over the energy levels in the QWs and barrier layers (Table 1), it can be seen that narrow QWs have considerably poorer confinement of charge carriers (as a rule, of electrons, due to their small effective mass). Even in the case of a deep QW, up to one-tenth of the

**Table 1.** Carrier distribution (%) over energy levels in a GaAs QW and $Al_{0.4}Ga_{0.6}As$ barrier region.

| Level in the QW | QW width | | |
|---|---|---|---|
| | 2–3 nm | 6–7 nm | 11–12 nm |
| 1 | 90–97 | 99.5 | 86–91 |
| 2 | – | 0.5 | 8–13 |
| 3 | – | – | 1 |
| Levels in the barrier layers | 3–10 | 0 | 0 |

It is also worth noting that another characteristic feature of narrow QWs is a stronger penetration of wave functions of electrons and holes into the barrier material. If its quality is poorer and/or there is a high rate of recombination on heterojunctions, this will lead to an increase in the contribution of all nonradiative recombination currents to the threshold current density according to formula (2) [32].

The Auger recombination current density is often neglected because in most theoretical studies the coefficients of Auger processes ($C_{Auger}$) for electrons and holes in the GaAs/AlGaAs material system are taken to be $10^{-30}$ to $10^{-31}$ cm$^6$ s$^{-1}$. At the same time, if we take into account that, in a number of experiments, these coefficients were $\sim 10^{-29}$ cm$^6$ s$^{-1}$ [33, 34] (they can increase with injected carrier concentration $N_{inject}$ and temperature), the threshold Auger recombination current density calculated as described in Ref. [9],

$$J_{\mathrm{Auger}} = qN_{\mathrm{inject}}^{3}L_z\, C_{\mathrm{Auger}}, \qquad (6)$$

can reach about 30 A cm$^{-2}$.

An analogous situation is possible in the case of the current density due to recombination on heterojunctions, where zero recombination velocity, impossible in practice, is used instead of $\upsilon_{\mathrm{interface}} \approx 50-450$ cm s$^{-1}$ [35–37].

For finally calculating the threshold current density, we should calculate the gain spectrum, which can be written in the general case as

$$g(E) = A\int M^2\rho(\epsilon)[f_{\mathrm{c}}(\epsilon) - f_{\mathrm{v}}(\epsilon)]\frac{\Delta\epsilon}{(\epsilon - E)^2 + \Delta\epsilon^2}\mathrm{d}\epsilon, \qquad (7)$$

where $g(E)$ is the material gain spectrum; the coefficient $A$ characterises the material of the active region; $M^2$ is the square of the matrix element determining the probability of the transition; $\rho(\epsilon)$ is the reduced density of states; $f_{\mathrm{c}}(\epsilon)$ and $f_{\mathrm{v}}(\epsilon)$ are the probabilities of the filling of states in the CB and VB; $E$ is the energy of the transition; and the parameter $\Delta\epsilon$ takes into account interband scattering broadening.

Since (7) contains terms related to the density of states, the variation of the threshold current density with QW width is similar to that in Figs 3 and 4. Like in the case of $J_{\mathrm{transp}}$, minimum values of $J_{\mathrm{th}}$ correspond to QW widths from 6 to 7 nm.

The absolute threshold current density can be further reduced by modifying the band structure, e.g. by doping the active region with an n-type impurity or subjecting the QW to mechanical compression/tension stress. In the former case, we concurrently shift the quasi Fermi levels in the CB and VB upwards, changing the initial degeneracies in these bands while maintaining the transparency condition fulfilled. In the latter, we change the band diagram by reducing the carrier effective mass in the VB and separating subbands of light and heavy holes. Producing stress is more preferable because, unlike n-type doping of QWs, it allows one to raise the material gain and, hence, the external differential efficiency [38].

Finally, let us analyse the effect of waveguide width and composition on the threshold current of LDs. The $\mathrm{Al}_x\mathrm{Ga}_{1-x}\mathrm{As}$ ($x = 0.1-0.5$) barrier material considered above was a waveguide layer, and the active region width was about 7 nm. As emitter layers in the laser heterostructure, we used a wide-band-gap $\mathrm{Al}_x\mathrm{Ga}_{1-x}\mathrm{As}$ composition with $x$ exceeding that in the waveguide layers by 0.2, which was necessary for efficient optical and electron confinement.

The threshold current density calculation results for heterostructures with a narrow (0.2–0.4 μm) and a broad (2.0–2.5 μm) waveguide for typical LD designs with a cavity length of 1 mm and stripe contact width of 100 μm demonstrate that, as the fraction $x$ of waveguide layers, i.e. the potential well depth, increases, the threshold current density decreases systematically due to more effective electron confinement in the QW. In the case of a broad waveguide, increasing $x$ from 0.10 to 0.25 leads to a sharper drop in $J_{\mathrm{th}}$ (from 700 to ~400 A cm$^{-2}$) than in the case of heterostructures with a narrow waveguide, where $J_{\mathrm{th}}$ decreases from 270 to ~200 A cm$^{-2}$. In the case of the deepest QWs (barrier material with $x = 0.1$), $J_{\mathrm{th}} = 180$ A cm$^{-2}$ for a narrow waveguide and 320 A cm$^{-2}$ for a broad one. In the general case, because of the large optical confinement factor in the active region of heterostructures with a narrow waveguide, the threshold current in lasers based on such heterostructures is markedly lower than that in lasers based on heterostructures with a broad waveguide. Moreover, calculations of output characteristics at elevated temperatures show that lasers based on structures with a narrow waveguide have larger $T_0$ and $T_1$ characteristic parameters, which is extremely important in designing laser emitters with improved temperature stability [15, 23].

The use of a similar approach to reducing the threshold current density for optimising the width and composition of the quantum confinement region, as well as the width and composition of waveguide layers based on the (Al)GaAs/AlGaAs material system, allowed the output parameters of devices to be substantially improved. In particular, reducing the threshold current by 10% to 12% and raising efficiency by 10% to 15% allowed high efficiencies (at a level of 70% and 62%) of laser bars and arrays, respectively, to be obtained [26, 39].

In conclusion, note that we have optimised an (Al)GaAs/AlGaAs heterostructure with a quantum confinement region in order to improve output characteristics of LDs. Determining the position of the quasi Fermi levels in an unstrained QW upon carrier injection with allowance for the filling of the light and heavy hole subbands in the VB and energy minima in the CB and calculating the laser mode gain, we have proposed an algorithm for optimising the active region geometry (width and depth). Reducing the threshold carrier concentration and carrier leakage to the barrier layers makes it possible to reduce the internal optical loss, increase differential efficiency and, as a consequence, improve the efficiency of semiconductor emitters.

## References


1. Klotzkin David J. *Introduction to Semiconductor Lasers for Optical Communications* (New York: Springer-Verlag, 2014).
2. Diehl R. *High-power Diode Lasers. Fundamentals, Technology, Applications* (Berlin–Heidelberg: Springer-Verlag, 2000).
3. Piprek J. *Semiconductor Optoelectronic Devices. Introduction to Physics and Simulation* (Amsterdam: Academic Press, 2003).
4. Slipchenko S.O., Vinokurov D.A., Pikhtin N.A., Sokolova Z.N., Stankevich A.L., Tarasov I.S., Alferov Zh.I. *Semiconductors*, **38**, 1430 (2004) [*Fiz. Tekh. Poluprovodn.*, **38**, 1477 (2004)].
5. Ladugin M.A., Koval' Yu.P., Marmalyuk A.A., Petrovskii V.A., Bagaev T.A., Andreev A.Yu., Padalitsa A.A., Simakov V.A. *Quantum Electron.*, **43**, 407 (2013) [*Kvantovaya Elektron.*, **43**, 407 (2013)].
6. Marmalyuk A.A., Ladugin M.A., Andreev A.Yu., Telegin K.Yu., Yarotskaya I.V., Meshkov A.S., Konyaev V.P., Sapozhnikov S.M., Lebedeva E.I., Simakov V.A. *Quantum Electron.*, **43**, 895 (2013) [*Kvantovaya Elektron.*, **43**, 895 (2013)].
7. Pikhtin N.A., Slipchenko S.O., Sokolova Z.N., Tarasov I.S. *Semiconductors*, **36**, 344 (2002) [*Fiz. Tekh. Poluprovodn.*, **36**, 364 (2002)].
8. Tsang W. *Appl. Phys. Lett.*, **40**, 217 (1982).
9. Zory P.S. Jr (Ed.) *Quantum Well Lasers* (San Diego: Academic Press, 1993).
10. Arakawa Y., Sakaki H., Nishioka M., Yoshino J., Kamiya T. *Appl. Phys. Lett.*, **46**, 519 (1985).
11. Wang P., Lee K.K., Yao G., Chen Y.C., Waters R.G. *Appl. Phys. Lett.*, **56**, 2083 (1990).
12. Chen T.R., Eng L.E., Zhuang Y.H., Yariv A. *Appl. Phys. Lett.*, **56**, 1002 (1990).
13. Murashova A.V., Vinokurov D.A., Pikhtin N.A., Slipchenko S.O., Shamakhov V.V., Vasil'eva V.V., Kapitonov V.A., Leshko A.Yu., Lyutetskii A.V., Nalet T.A., Nikolaev D.N., Stankevich A.L., Fetisova N.V., Tarasov I.S., Kim Y.S., Kang D.H., Lee C.Y. *Semiconductors*, **42**, 862 (2008) [*Fiz. Tekh. Poluprovodn.*, **42**, 882 (2008)].
14. Chen H.Z., Ghaffari A., Morkoç H., Yariv A. *Appl. Phys. Lett.*, **51**, 2094 (1987).

15. Ladugin M.A., Lyutetskii A.V., Marmalyuk A.A., Padalitsa A.A., Pikhtin N.A., Podoskin A.A., Rudova N.A., Slipchenko S.O., Shashkin I.S., Bondarev A.D., Tarasov I.S. *Semiconductors*, **44**, 1370 (2010) [*Fiz. Tekh. Poluprovodn*., **44**, 1417 (2010)].
16. Hersee S.D., de Cremoux B., Duchemin J.P. *Appl. Phys. Lett*., **44**, 476 (1984).
17. Lo Y.C., Hsieh K.Y., Kolbas R.M. *Appl. Phys. Lett*., **52**, 1853 (1988).
18. Andreev A.Yu., Zorina S.A., Leshko A.Yu., Lyutetskii A.V., Marmalyuk A.A., Murashova A.V., Nalet T.A., Padalitsa A.A., Pikhtin N.A., Sabitov D.R., Simakov V.A., Slipchenko S.O., Telegin K.Yu., Shamakhov V.V., Tarasov I.S. *Semiconductors*, **43**, 519 (2009) [*Fiz. Tekh. Poluprovodn*., **43**, 543 (2009)].
19. Sugimura A. *IEEE J. Quantum Electron*., **20**, 336 (1984).
20. Arakawa Y., Yariv A. *IEEE J. Quantum Electron*., **21**, 1666 (1985).
21. Kasemset D., Hong C.-S., Patel N.B., Dapkus P.D. *IEEE J. Quantum Electron*., **19**, 1025 (1983).
22. Saint-Cricq B., Lozes-Dupuy F., Vassilieff G. *IEEE J. Quantum Electron*., **22**, 625 (1986).
23. Marmalyuk A.A., Ladugin M.A., Andreev A.Yu., Telegin K.Yu., Yarotskaya I.V., Meshkov A.S., Konyaev V.P., Sapozhnikov S.M., Lebedeva E.I., Simakov V.A. *Quantum Electron*., **43**, 895 (2013) [*Kvantovaya Elektron*., **43**, 895 (2013)].
24. Svelto O. *Principles of Lasers* (New York: Plenum, 1998; St. Petersburg: Lan', 2008).
25. Dragunov V.P., Neizvestnyi I.G., Gridchin V.A. *Osnovy nanoelektroniki: Uchebnoe posobie* (Principles of Nanoelectronics: A Learning Guide) (Novosibirsk: NGTU, 2000).
26. Ladugin M.A., Marmalyuk A.A., Padalitsa A.A., Bagaev T.A., Andreev A.Yu., Telegin K.Yu., Lobintsov A.V., Davydova E.I., Sapozhnikov S.M., Danilov A.I., Podkopaev A.V., Ivanova E.B., Simakov V.A. *Quantum Electron*., **47**, 291 (2017) [*Kvantovaya Elektron*., **47**, 291 (2017)].
27. Shichijo H., Kolbas R.M., Holonyak N. Jr. *Solid State Commun*., **27**, 1029 (1978).
28. Tsai C.-Y., Tsai C.-Y., Lo Y.-H., Spencer R.M., Eastman L.F. *IEEE J. Sel. Top. Quantum Electron*., **1**, 316 (1995).
29. Brum J.A., Bastard G. *Phys. Rev. B*, **33**, 1420 (1986).
30. Haverkort J.E.M., Blom P.W.M., Van Hall P.J., Claes J., Wolte J.H. *Phys. Status Solidi B*, **188**, 139 (1995).
31. Sokolova Z.N., Tarasov I.S., Asryan L.V. *Semiconductors*, **45**, 1494 (2011) [*Fiz. Tekh. Poluprovodn*., **45**, 1553 (2011)].
32. Hariz A., Dapkus P.D., Lee H.C., Menu E.P., DenBaars S.P. *Appl. Phys. Lett*., **54**, 635 (1989).
33. Strauss U., Rühle W.W., Köhler K. *Appl. Phys. Lett*., **62**, 55 (1993).
34. Lush G.B., MacMillan H.F., Keyes B.M., Levi D.H., Melloch M.R., Ahrenkiel R.K., Lundstrom M.S. *J. Appl. Phys*., **72**, 1436 (1992).
35. Wolford D.J., Gilliland G.D., Kuech T.F., Klem J.F., Hjalmarson H.P., Bradley J.A., Tsang C.F., Martinsen J. *Appl. Phys. Lett*., **64**, 1416 (1994).
36. Viswanath A.K. *Handbook of Surfaces and Interfaces of Materials* (San Diego: Academic Press, 2001).
37. Pavesi L., Guzzi M. *J. Appl. Phys*., **75**, 4779 (1994).
38. Coldren L.A., Corzine S., Mashanovitch M. *Diode Lasers and Photonic Integrated Circuits* (Hoboken, New Jersey: John Wiley & Sons Inc., 2012).
39. Ladugin M.A., Marmalyuk A.A., Padalitsa A.A., Telegin K.Yu., Lobintsov A.V., Sapozhnikov S.M., Danilov A.I., Podkopaev A.V., Simakov V.A. *Quantum Electron*., **47**, 693 (2017) [*Kvantovaya Elektron*., **47**, 693 (2017)].